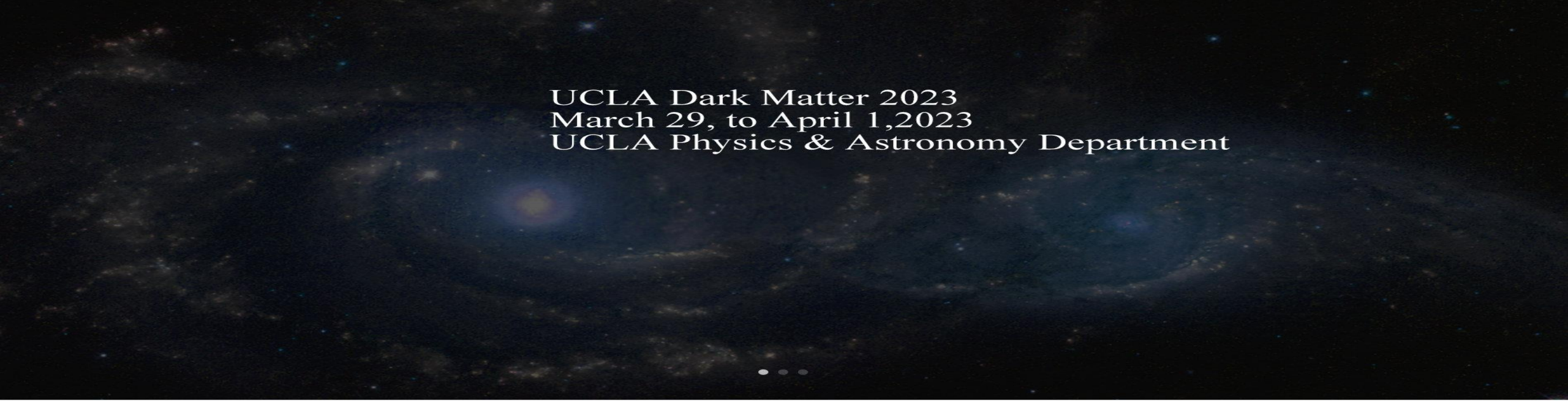

Constraints on Spin dependent and Spin Independent Dark Matter-Electron Scattering

Mukesh Kumar Pandey
Department of Physics,
National Dong Hwa University
Taiwan

Co-author:

Chih-Pang Wu (University of Montreal, Canada), Lakhwinder Singh (CUSB, India), Chen-Pang Liu, Hsin-Chang Chi (NDHU, Taiwan), Jiunn-Wei Chen (NTU, Taiwan), Henry T. Wong (IOP, Academia Sinica, TEXONO Collaboration, Taiwan)

What We've Done in This Work

- **Atomic approach is fully relativistic**
- Spin-Dependent DM-e interaction is considered together with Spin-Independent interaction, to provide a more comprehensive understanding about the nature of DM & its interaction.
- We set a limit on the SD & SI DM-e cross sections at leading order with state-of-the-arts atomic many-body calculations and current best experiment data.
- One can differentiate the shape of SD and SI recoil spectra at high energies when spin obit interaction becomes more relevant.

References:

1. Mukesh K. Pandey et al ., Phys. Rev. D 102, 123025 (2020); arXiv:1812.11759.
2. C.-P. Liu et al., PHYS. REV. D 106, 063003 (2022); arXiv:2106.16214

Outline of the talk

1. **Motivation**
2. **Why Atomic Physics ?**
3. **Brief outline about Theoretical approach**
4. **Result and discussions**
5. **Conclusion**

Why Atomic Physics?

Why Atomic Physics?

- Energy scales: Atomic (~ eV) Reactor neutrino (~ MeV) WIMP (~ GeV)
- Neutrino: NNM atomic ionization signal larger at lower energy scattering (current Ge detector threshold 0.1 keV)
- DM: direct detection, velocity slow (~ 1/1000), max energy 1 keV for mass 1 GeV DM.

Opportunity: Applying atomic physics at keV (low for nuclear physics but high for atomic physics)

Brief outline about Theoretical approach

EFT DM-matter Lagrangian

Refs: Fan et. al., JCAP11(2010) 042; Fitzpatrick, et. al., JCAP02(2013) 004

- Leading-Order

SI SD

$$\mathcal{L}_{\text{int}}^{(\text{LO})} = \sum_{f=e,p,n} \left\{ c_1^{(f)} (\chi^\dagger \chi)(f^\dagger f) + c_4^{(f)} (\chi^\dagger \vec{S}_\chi \chi) \cdot (f^\dagger \vec{S}_f f) \right. \quad \leftarrow \text{SR}$$

$$\left. + d_1^{(f)} \frac{1}{q^2} (\chi^\dagger \chi)(f^\dagger f) + d_4^{(f)} \frac{1}{q^2} (\chi^\dagger \vec{S}_\chi \chi) \cdot (f^\dagger \vec{S}_f f) \right\} \quad \leftarrow \text{LR}$$

where χ and f denote the DM and fermion fields, respectively, S_χ, S_f are their spin operators (scalar DM particles have null S_χ), the DM 3-momentum transfer |q| depends on the DM energy transfer T

- **c_1 and c_4 called as contact interaction, and it is an energy-independent constant**
- **d_1 and d_4 called as the long rang interaction, and it is an energy-dependent constant**

DM-Atom ionization differential Cross Sections

Example:-
The differential DM-atom ionization cross section in the laboratory frame through the LO, SI DM-electron interaction

$$\frac{d\sigma}{dT} = \frac{1}{2\pi v_\chi^2} \int dq q \left[\left| c_1 + \frac{d_1}{q^2} \right|^2 \right] R(T, q),$$

Where V_χ is the velocity of the DM particle.

Response Function

$$R(T,\theta) = 4\pi \sum_{i=1}^{Z} \int d^3p_i \, | \langle \mathrm{A}^+, e^- || e^{i\frac{\mu}{m_e}\vec{q}.\vec{r}_i} || \mathrm{A} \rangle |^2$$
$$\times \, \delta(T - E_{B_i} - \frac{\vec{q}^2}{2M} - \frac{\vec{p_i}^2}{2\mu}) \, ,$$

- The full information of how the detector atom responds to the incident DM particle is encoded in the response function

- Biggest Challenge: Many-body wave functions for the initial and final states

- ***R(T, ϑ)*** is evaluated by well-benchmarked procedure based on an *ab-inito* method, the (multi-configuration) relativistic random phase approximation, (MC)RRPA.

- To expedite the computation, we performed (MC)RRPA calculations only for selected data points, and the full computation is done with an additional approximation: the frozen-core approximation (FCA).

The FCA has a discrepancy less than 20% for all our calculations.

Response Function

In the NR-IPA scheme, the SI response function

$$\mathcal{R}_{\mathrm{SI}}^{(\mathrm{ion})}(T,q) = \sum_{k_f l_f j_f} \sum_{n_i l_i j_i} \sum_{L=0} 4\pi |\langle k_f l_f j_f || j_L(qr) Y_L(\Omega_r) || n_i l_i j_i \rangle|^2 \delta(E\ldots),$$

$$= \sum_{k_f l_f} \sum_{n_i l_i} \sum_{L=0} 2[l_f]^2 [l_i]^2 [L]^2 \begin{pmatrix} l_f & L & l_i \\ 0 & 0 & 0 \end{pmatrix}^2 \langle k_f l_f | j_L(qr) | n_i l_i \rangle^2_{(\mathrm{NR})} \delta(E\ldots),$$

$$\mathcal{R}_{\mathrm{SD}}^{(\mathrm{ion})}(T,q) = \sum_{k_f l_f} \sum_{n_i l_i} 2[l_f]^2 [l_i]^2 \left\{ [1]^2 \begin{pmatrix} l_f & 0 & l_i \\ 0 & 0 & 0 \end{pmatrix}^2 \right.$$

$$\left. + \sum_{L=1} ([L]^2 + [L-1]^2 + [L+1]^2) \begin{pmatrix} l_f & L & l_i \\ 0 & 0 & 0 \end{pmatrix}^2 \right\} \langle k_f l_f | j_L(qr) | n_i l_i \rangle^2_{(\mathrm{NR})} \delta(E\ldots)$$

$$= \sum_{k_f l_f} \sum_{n_i l_i} \sum_{L=0} 6[l_f]^2 [l_i]^2 [L]^2 \begin{pmatrix} l_f & L & l_i \\ 0 & 0 & 0 \end{pmatrix}^2 \langle k_f l_f | j_L(qr) | n_i l_i \rangle^2_{(\mathrm{NR})} \delta(E\ldots)$$

$$= 3\mathcal{R}_{\mathrm{SI}}^{(\mathrm{ion})}(T,q),$$

Average Velocity-weighted differential

$$\frac{d\langle\sigma v_\chi\rangle}{dT} = \int_{v_{\min}}^{v_{\max}} d^3 v_\chi f(\vec{v}_\chi) v_\chi \frac{d\sigma}{dT}$$

The average velocity-weighted differential is folded to the conventional Maxwell-Boltzmann velocity distribution $f(\vec{v}_\chi)$

With escape velocity V_{esc} = 544 km/s , circular velocity V_0 = 220 km/s, and averaged Earth relative velocity V_E= 232 km/s.

The maximum DM velocity seen from the Earth is $V_{max} = V_{esc} + V_E$, and the minimum $v_{\min} = \sqrt{2T/m_\chi}$ is to guarantee enough kinetic energy.

Results we've got:

Important Lessons

- Benchmark, benchmark, benchmark.
- Relativistic and MB effects are important.
- Spin-orbit interaction is critical in SD responses.

Benchmark: Ge Photoionization

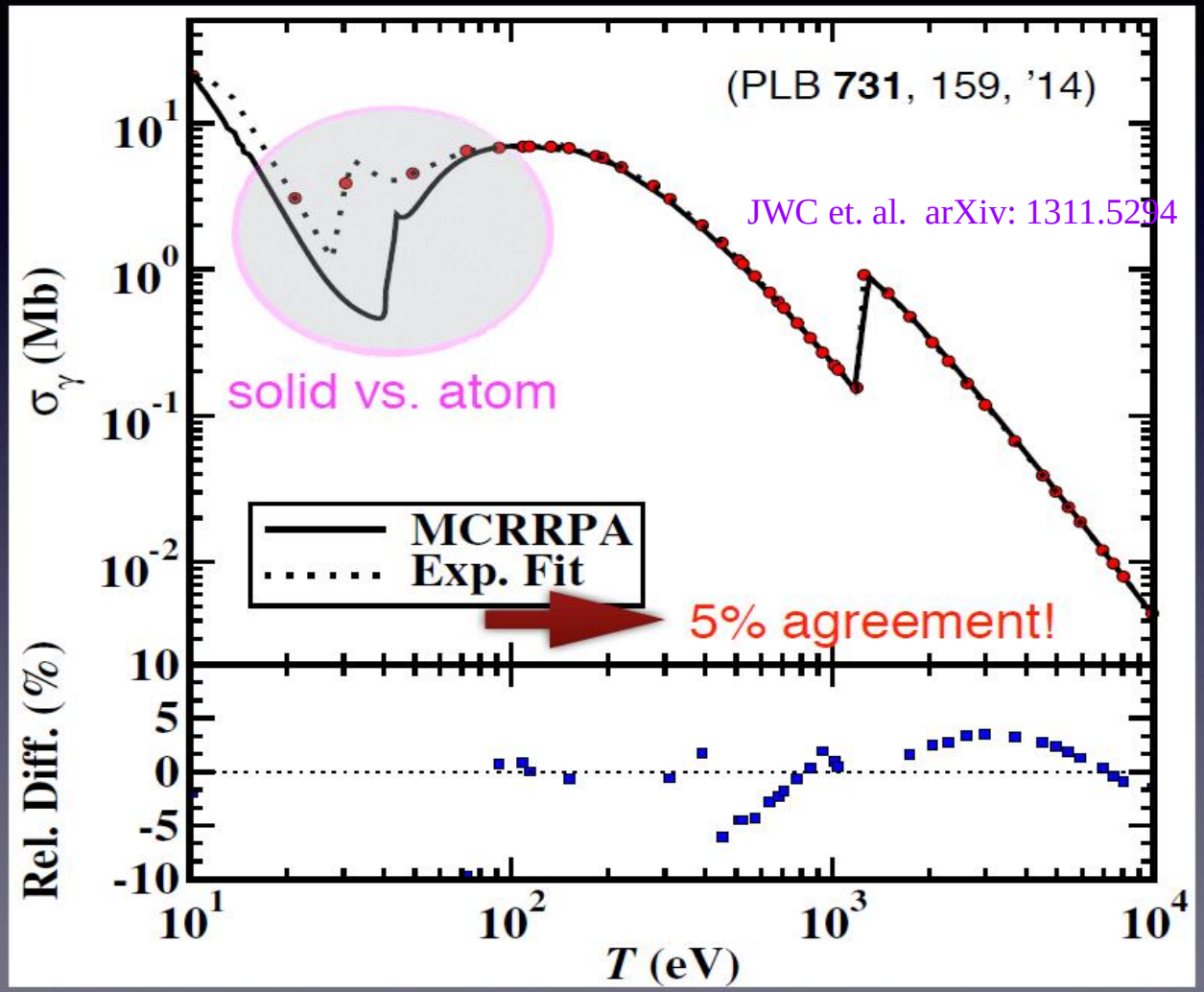

- The main error are located at 10 to 100 eV for Ge case. It may come from the solid effects but in our calculations where we only consider one Ge atom.

Benchmark: Xe Photoionization

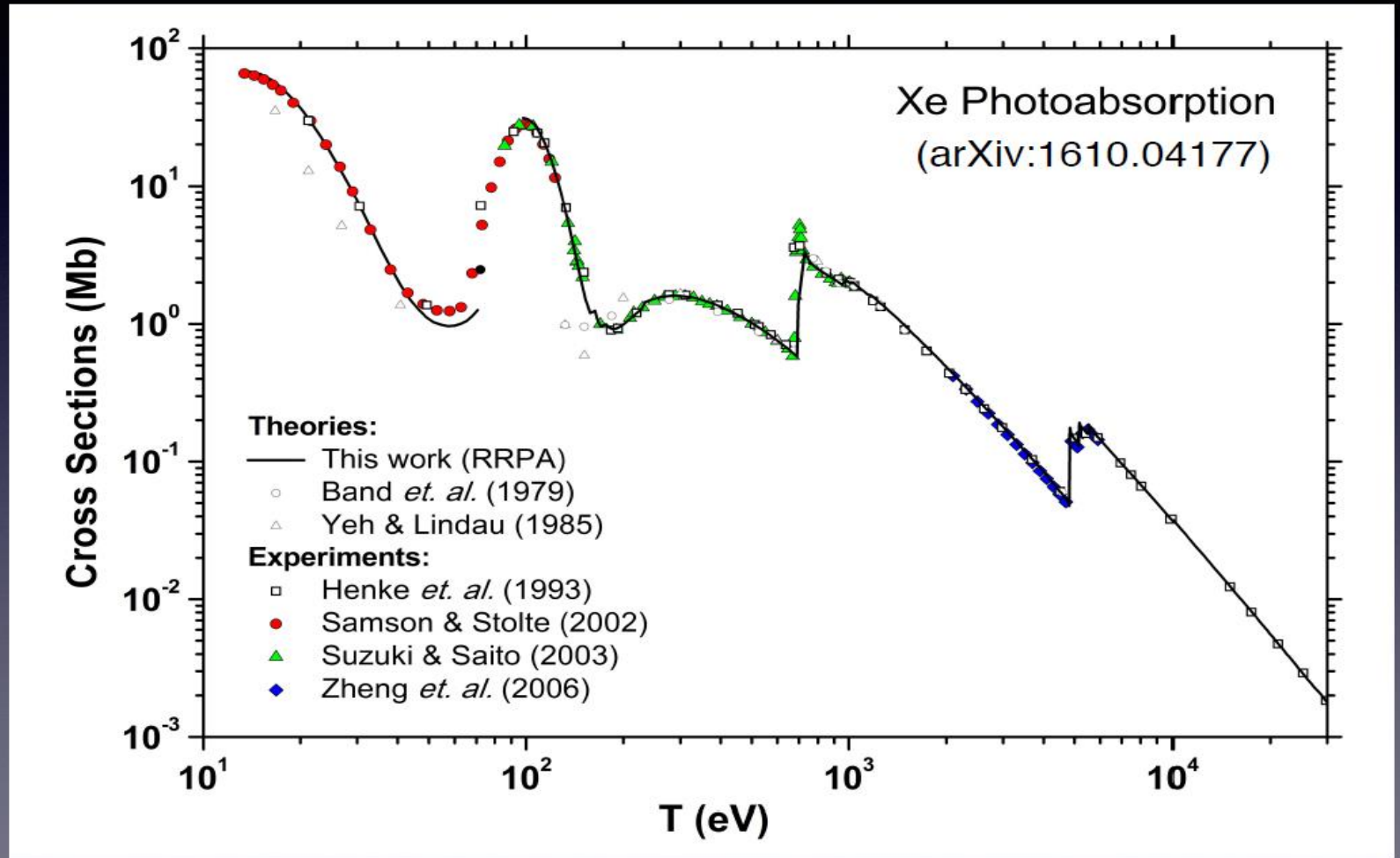

Averaged velocity-weighted differential cross sections

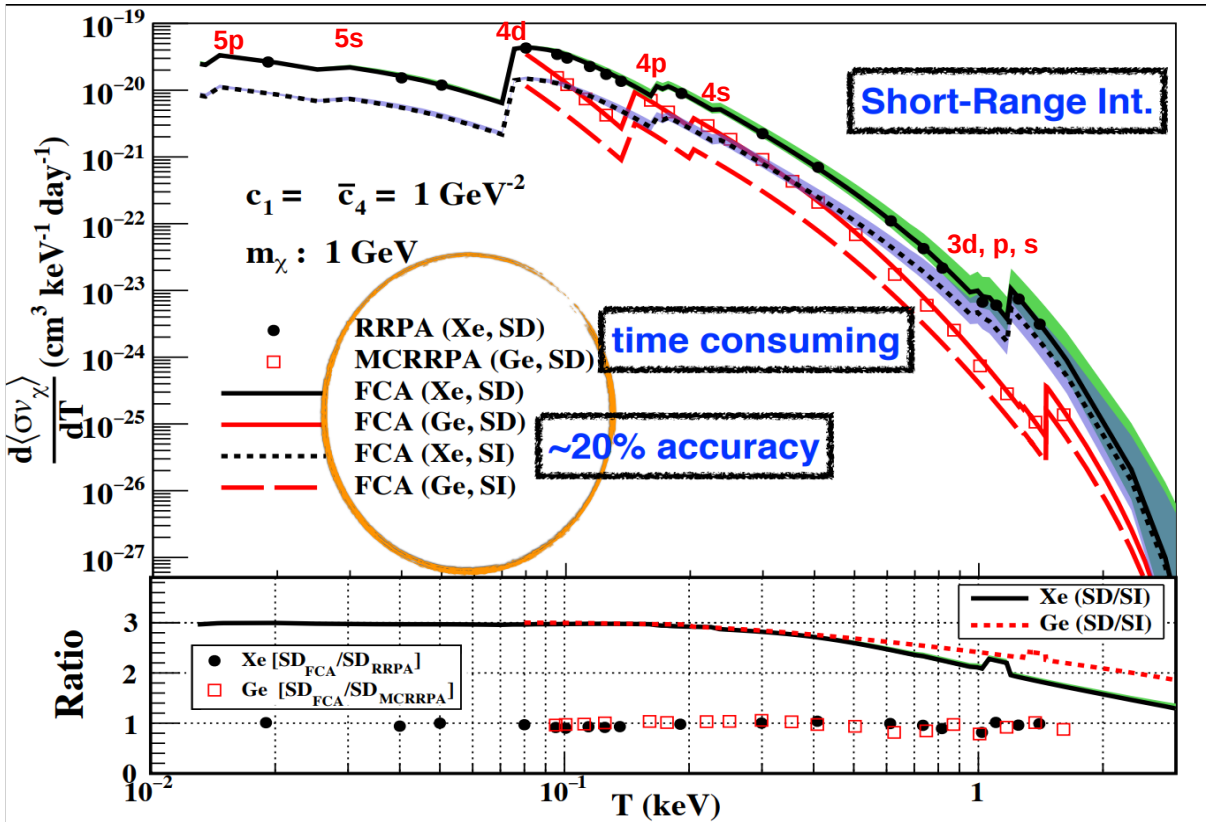

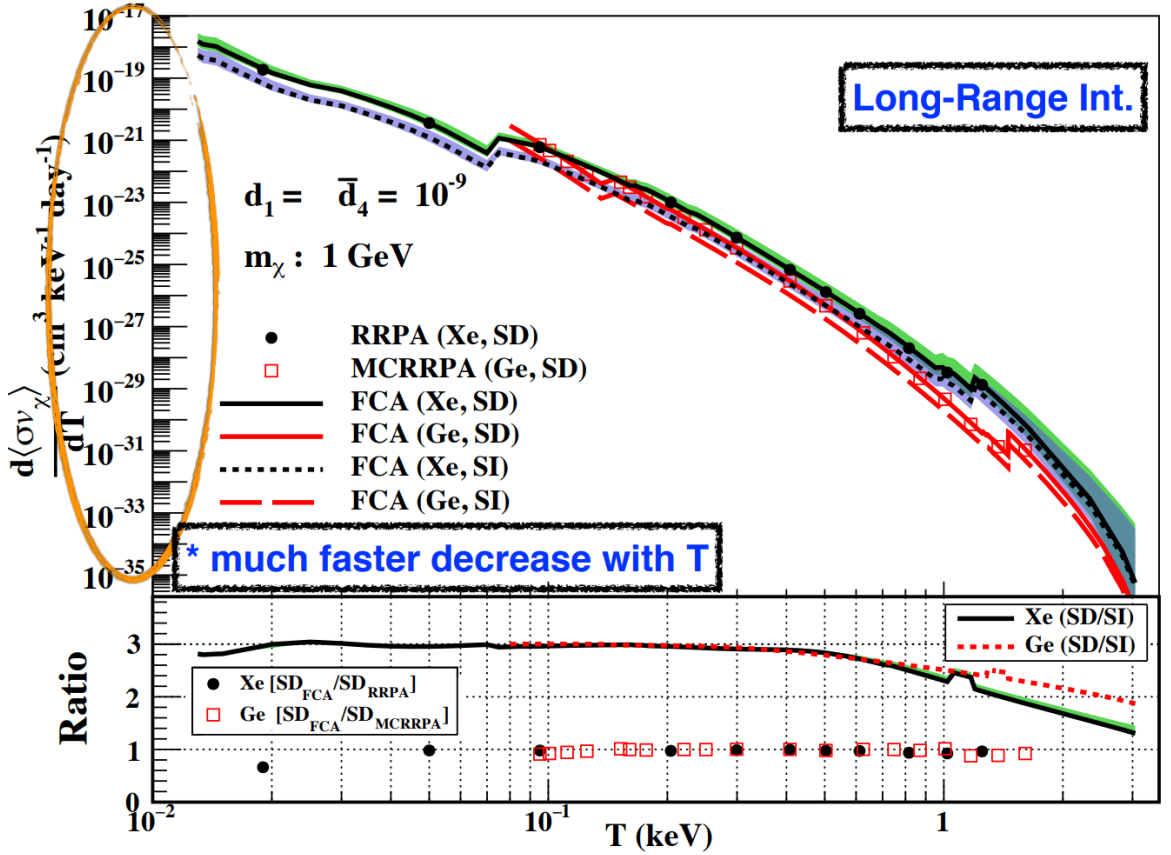

❖ **In these figure, we show some results of Averaged velocity-weighted differential cross sections for ionization of Ge and Xe atoms by LDM of 1 GeV mass with the effective short-range (Left) and long-range (Right) interactions**

Important observations

- **First,** the sharp edges correspond to ionization thresholds of specific atomic shells.
- **Second,** away from these edges, the comparison between Ge and Xe cases, Xe has a larger cross section.

How to distinguish the SD/SI signals?

Averaged velocity-weighted differential cross sections

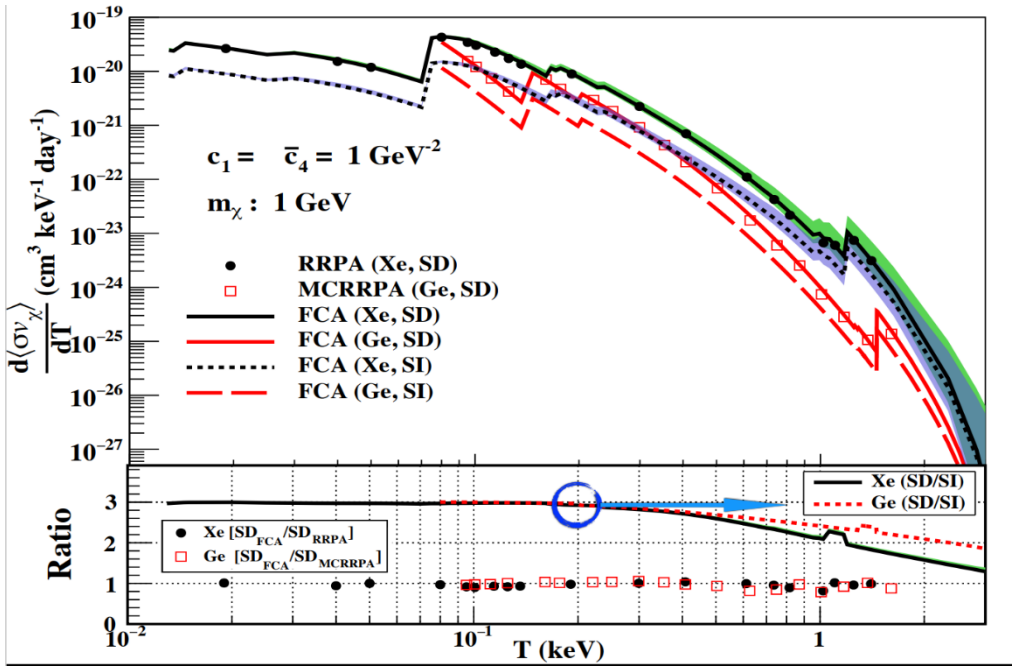

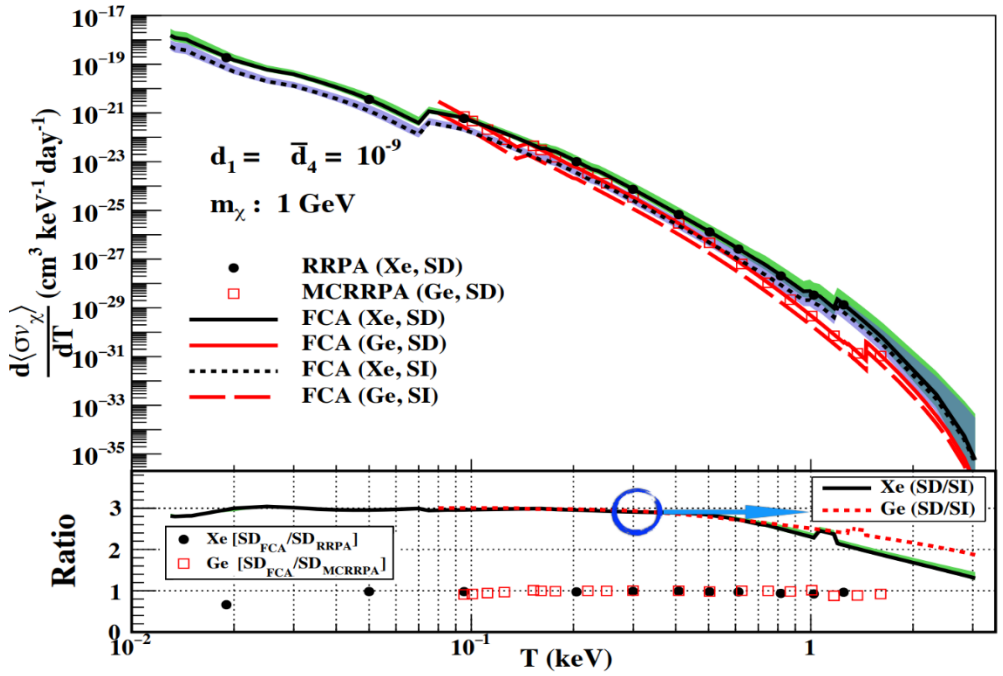

Important observations

- At T $\lesssim$ 200 eV, the scaling relation $\bar{\xi} \approx 3$ works well for both xenon and germanium.
- The scaling deviation starts to grow as T increases, and the larger deviations in xenon than germanium demonstrates the effects of a stronger SOI in an atom of higher Z.
- **Therefore this is very clear that, in nonrelativistic limit, we can't distinguish the SD and SI recoil energy spectra.**

- **However, relativistic calculations show the scaling starts to break down at a few hundreds of eV, where the spin-orbit effects become sizable.**

Exclusion Plot on SI DM-electron

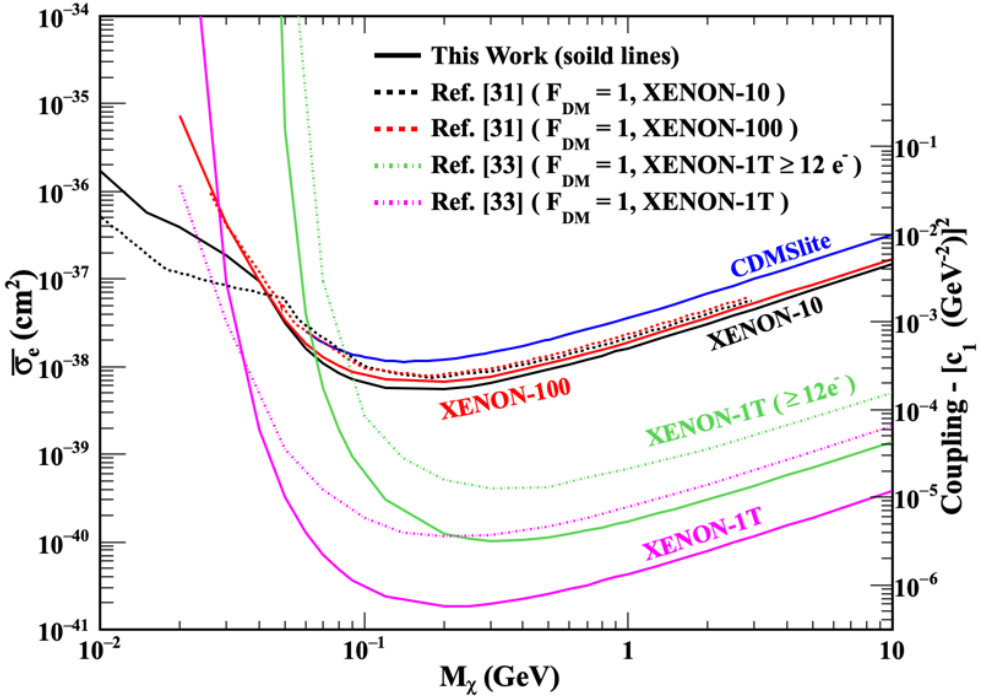

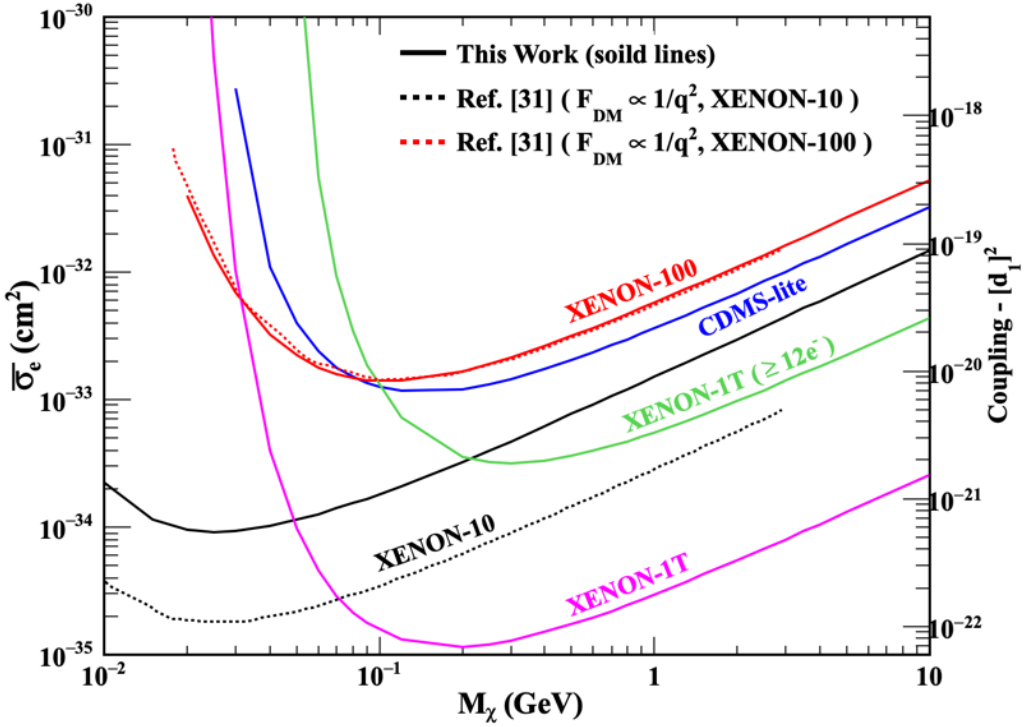

- In the DM mass range of 0.1–10 GeV, the best limits set by the XENON1T experiment

- In Fig, the exclusion limits derived in Refs. [31,33], using the same xenon data sets, are compared. The differences in the overall exclusion curves are obvious and most likely of theoretical origins.

[31] R. Essig, T. Volansky, and T.-T. Yu, Phys. Rev. D 96, 043017 (2017).
[33]E. Aprile et al. (XENON Collaboration), Phys. Rev. Lett. 123, 251801 (2019)

Exclusion Plot on SD DM-electron

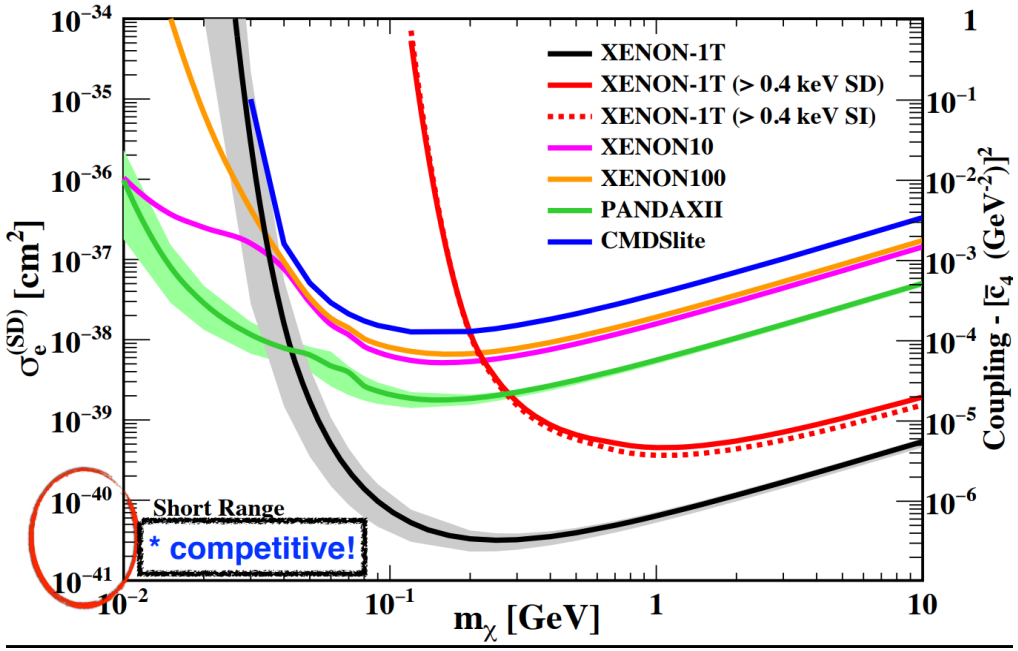

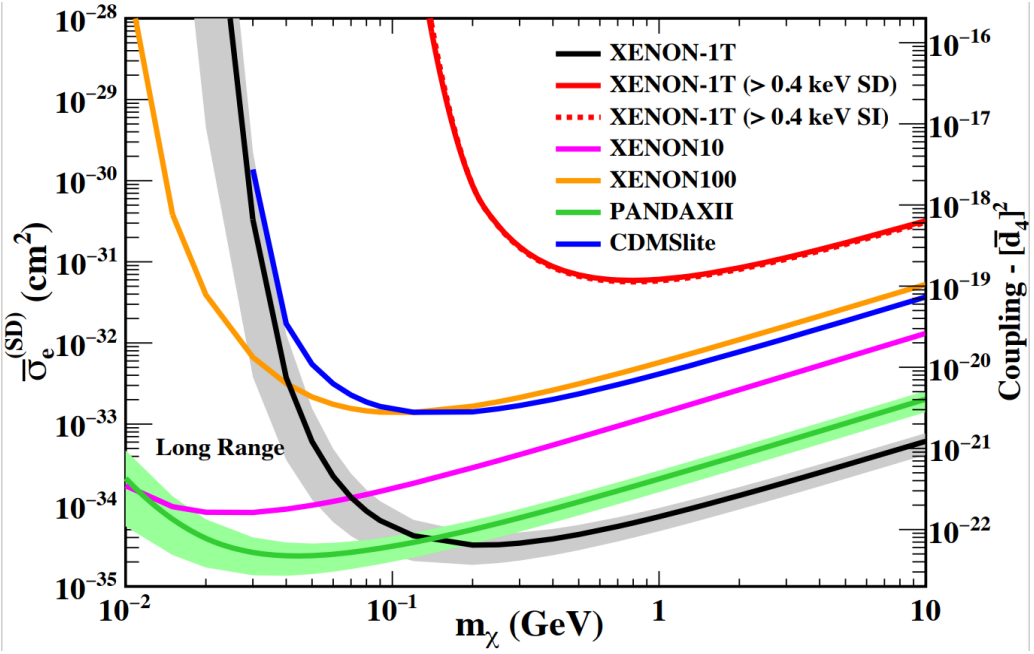

- In the DM mass range of 0.1–10 GeV, the best limits set by the XENON1T experiment: $\sigma_e^{SD} < 10^{-41}$–10^{-40} cm^2, are comparable to the ones drawn on DM-neutron and DM-proton at slightly bigger DM masses.

- We also explore the impact of uncertainties in the DM velocity spectrum, by vary Vesc; V_0; V_E in the range of… .

$$(220 \pm 18, 580 \pm 63, 242 \pm 10)\ \mathrm{km/s}.$$

The changes are illustrated by bands in Fig. for the xenon case

Summary

- In summary, we conclude the scattering cross section of sub-GeV dark matter off atoms depends sensitively on atomic structure.
- Our atomic approach is fully relativistic, and the frozen-core approximation is well benchmarked by (MC)RRPA (a truly many-body approach). The theoretical uncertainty of our results is estimated to be about 20%
- For LDM-electron interactions, atomic transition plays an important role because ionization channel dominates the scattering process
- SD DM-electron interactions are important to unravel the nature of DM and its interactions with matter.
- One can differentiate the shape of SD and SI recoil spectra at high energies when spin obit interaction becomes more relevant.

Soon, we are going to provide Data of Atomic Response function for DM and Atomic interaction on our group web site.

https://web.phys.ntu.edu.tw/~jwc/DarkMatterandNeutrinoGroup/

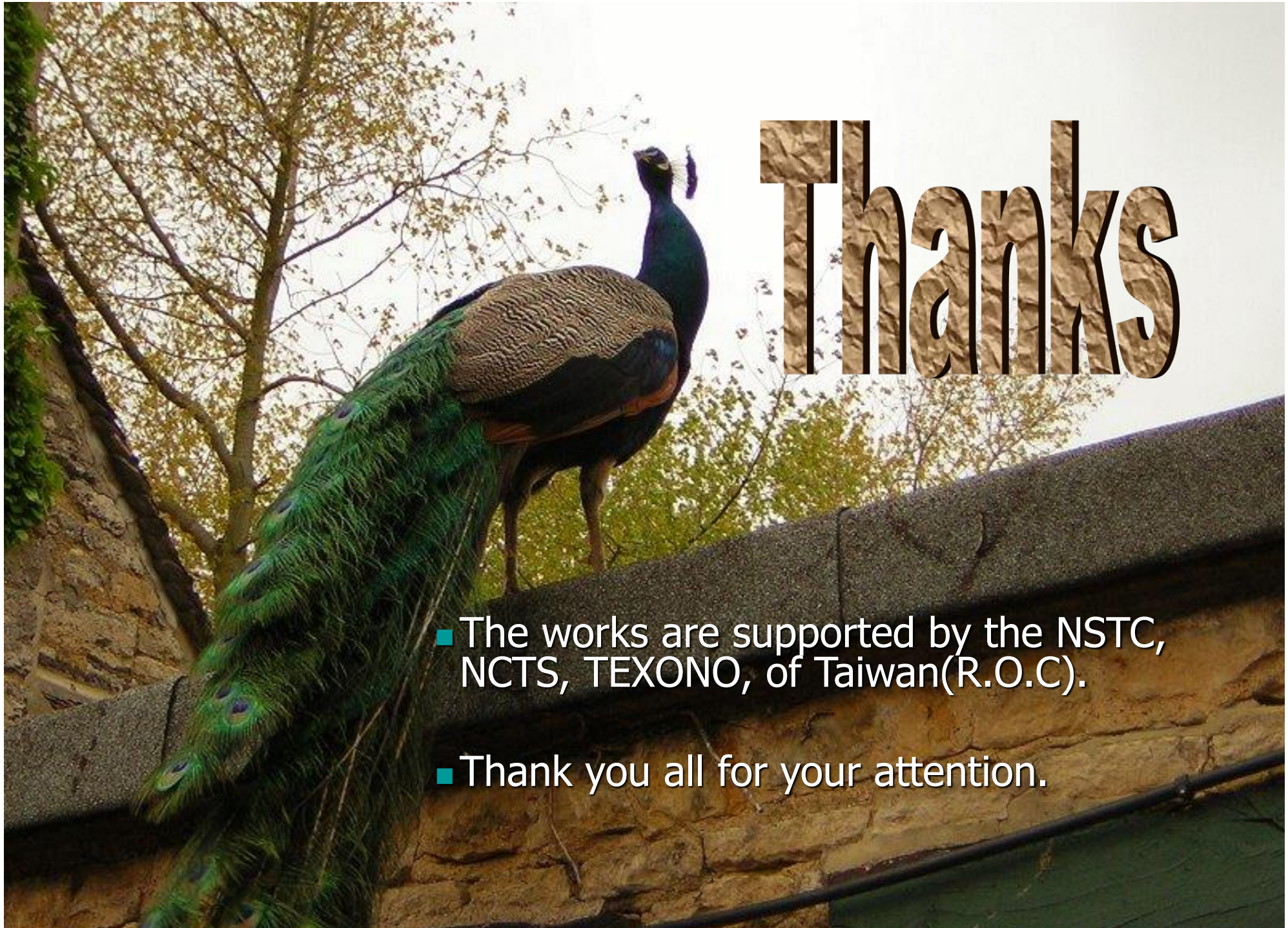

- The works are supported by the NSTC, NCTS, TEXONO, of Taiwan(R.O.C).

- Thank you all for your attention.

Backup slides

Response Function

In the NR-IPA scheme, the SI response function

$$\mathcal{R}_{\mathrm{SI}}^{(\mathrm{ion})}(T,q) = \sum_{k_f l_f j_f} \sum_{n_i l_i j_i} \sum_{L=0} 4\pi |\langle k_f l_f j_f || j_L(qr) Y_L(\Omega_r) || n_i l_i j_i \rangle|^2 \delta(E\ldots),$$

$$= \sum_{k_f l_f} \sum_{n_i l_i} \sum_{L=0} 2[l_f]^2 [l_i]^2 [L]^2 \begin{pmatrix} l_f & L & l_i \\ 0 & 0 & 0 \end{pmatrix}^2 \langle k_f l_f | j_L(qr) | n_i l_i \rangle^2_{(\mathrm{NR})} \delta(E\ldots),$$

$$\mathcal{R}_{\mathrm{SD}}^{(\mathrm{ion})}(T,q) = \sum_{k_f l_f} \sum_{n_i l_i} 2[l_f]^2 [l_i]^2 \left\{ [1]^2 \begin{pmatrix} l_f & 0 & l_i \\ 0 & 0 & 0 \end{pmatrix}^2 \right.$$

$$\left. + \sum_{L=1} ([L]^2 + [L-1]^2 + [L+1]^2) \begin{pmatrix} l_f & L & l_i \\ 0 & 0 & 0 \end{pmatrix}^2 \right\} \langle k_f l_f | j_L(qr) | n_i l_i \rangle^2_{(\mathrm{NR})} \delta(E\ldots)$$

$$= \sum_{k_f l_f} \sum_{n_i l_i} \sum_{L=0} 6[l_f]^2 [l_i]^2 [L]^2 \begin{pmatrix} l_f & L & l_i \\ 0 & 0 & 0 \end{pmatrix}^2 \langle k_f l_f | j_L(qr) | n_i l_i \rangle^2_{(\mathrm{NR})} \delta(E\ldots)$$

$$= 3\mathcal{R}_{\mathrm{SI}}^{(\mathrm{ion})}(T,q),$$

Comparisons of expected event numbers as a function of ionized electron number

To further trace the main origin of this discrepancy, we performed two additional sets of calculations:

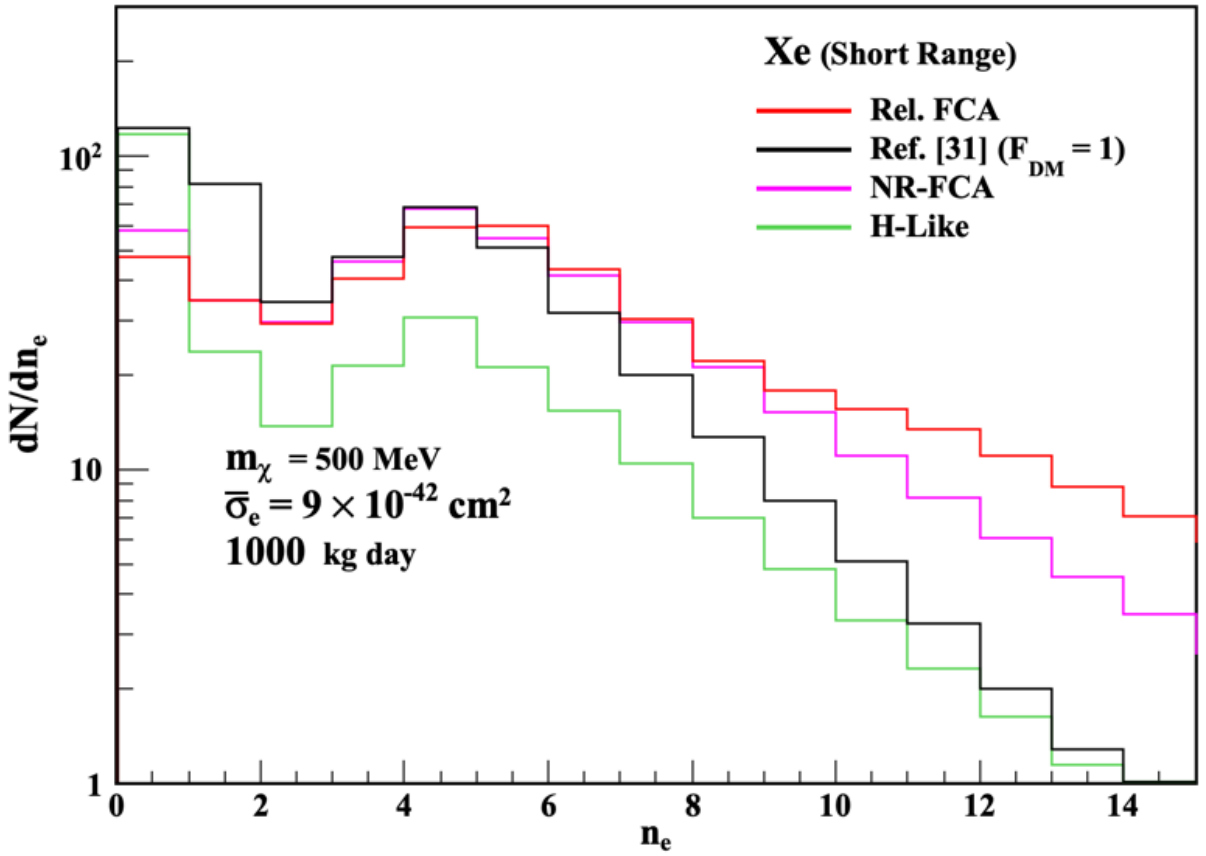

Comparisons of expected event numbers as a function of ionized electron number derived in this work (relativistic FCA, red), nonrelativistic FCA (magenta), hydrogenlike approximation (green), and from Ref. [31] (black) for Xe detectors with 1000 kg-year exposure, assuming DM mass m_χ = 500 MeV, and DM-electron interaction strengths c1 = 5.28 × 10

The difference between the NR-FCA and Ref. [31] is most likely due to different formulations of the effective Coulomb potential felt by an ionized electron. We did find the results of Ref. [31] fall in between NRFCA and HLA, so perhaps is the reconstructed Coulomb potentials

MCRRPA Wave Functions

$$\Psi(t) = \sum_a C_a(t)\psi_a(t)$$

Normalization

$$\langle \Psi(t)|\Psi(t)\rangle = 1$$

$$\langle u_\alpha(t)|u_\beta(t)\rangle = \delta_{\alpha\beta}$$

$$\langle \psi_a(t)|\psi_b(t)\rangle = \delta_{ab}$$

Slater determinant

$u_\alpha(t)$

$$\sum_a C_a^\star(t)C_a(t) = 1\,,$$

time-dependent external perturbation:

$$V(t) = \sum_{i=1}^{N} v_+(\mathbf{r}_i)e^{-i\omega t} + \sum_{i=1}^{N} v_-(\mathbf{r}_i)e^{+i\omega t}$$

Multipole expansion

$$v_+ = \sum_{JM\lambda} v_{JM}^{(\lambda)}$$

$$C_a(t) = C_a + [C_a]_+ e^{-i\omega t} + [C_a]_- e^{+i\omega t} \ldots$$

$$u_\alpha(t) = u_\alpha + w_{\alpha+}e^{-i\omega t} + w_{\alpha-}e^{+i\omega t} + \ldots$$

Transition amplitude:

$$T_J^{(\lambda)} = \sum_\alpha \left[\left\langle w_{\alpha+}\left|v_{JM}^{(\lambda)}\right|u_\alpha\right\rangle + \left\langle u_\alpha\left|v_{JM}^{(\lambda)}\right|w_{\alpha-}\right\rangle\right] + \sum_{ab}\left([C_a]_+^* C_b + C_a^*[C_b]_-\right)\left\langle \psi_a\left|v_{JM}^{(\lambda)}\right|\psi_b\right\rangle$$

The Transition Amplitude

$$\langle \Psi_f^{(-)} | v_+ | \Psi_i \rangle = \sum_\alpha \Lambda_\alpha (\langle w_{\alpha+} | v_+ | u_\alpha \rangle + \langle u_\alpha | v_+ | w_{\alpha-} \rangle)$$

$$+ \sum_{a,b} ([C_a]_+^\star C_b + C_a^\star [C_b]_-) \langle \psi_a | v_+ | \psi_b \rangle$$

The single-electron perturbing field:

$$v_+ = \int d^3x \; e^{i\vec{q}\cdot\vec{x}} \; l_\mu(\vec{x}) \, \hat{J}^\mu(\vec{x}) \,, \qquad v_- = v_+^\dagger$$

$$\mathbf{1} = \sum_{\lambda=0,\pm1} l_\lambda \, \hat{e}_\lambda^\dagger \qquad \hat{e} \text{ : basis a set of polarization vectors}$$

$$\hat{e}_{(\lambda=\pm1)} \; e^{i\vec{q}\cdot\vec{x}} = \sum_{J\geq1} i^J \sqrt{2\pi(2J+1)} \left\{ \mp j_J(kr) \mathcal{Y}_{JJ1}^\lambda - \frac{1}{k} \nabla \times [j_J(kr) \mathcal{Y}_{JJ1}^\lambda] \right\}$$

$$\hat{e}_{(\lambda=0)} \; e^{i\vec{q}\cdot\vec{x}} = \frac{-i}{k} \sum_{J\geq0} i^J \sqrt{4\pi(2J+1)} \; \nabla \, [j_J(kr) \, Y_{J0}]$$

Ab initio Theory for Atomic Ionization

MCDF: multiconfiguration Dirac-Fock method

Dirac-Fock method: $\psi(t)$ is a Slater determinant of one-electron orbitals $u_a(\vec{r},t)$

and invoke variational principle $\delta\left\langle\psi(t)\right| i\frac{\partial}{\partial t} - H - V_I(t)\left|\psi(t)\right\rangle = 0$

to obtain eigenequations for $u_a(\vec{r},t)$.

multiconfiguration: (for open shell atom) Approximate the many-body wave function $\Psi(t)$ by a superposition of configuration functions $\psi_\alpha(t)$

$$\Psi(t) = \sum_\alpha C_\alpha(t)\,\psi_\alpha(t)$$

Ge: 2 e^- in $4p$ (j = 1/2 or 3/2)

MCRRPA: multiconfiguration relativistic random phase approximation

RPA: Expand $u_a(\vec{r},t)$ into time-indep. orbitals in power of external potential

$$u_a(\vec{r},t) = e^{i\varepsilon_a t}\left[u_a(\vec{r}) + w_{a+}(\vec{r})e^{-i\omega t} + w_{a-}(\vec{r})e^{i\omega t} + \ldots\right]$$

$$C_a(t) = C_a + [C_a]_+ e^{-i\omega t} + [C_a]_- e^{i\omega t} + \ldots$$

Comparisons of expected event numbers as a function of ionized electron number

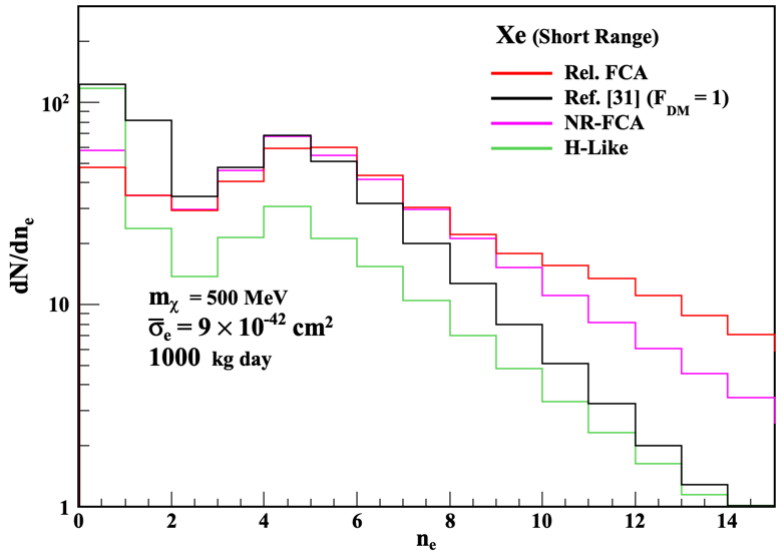

To further trace the main origin of this discrepancy, we performed two additional sets of calculations:

The larger the DM mass m_χ, the larger its kinetic energy and hence the increasing chance of higher energy scattering that produces more n_e. Therefore, our calculations yield tighter constraints on c_1 for heavier DM particles, but looser for lighter DM particles.

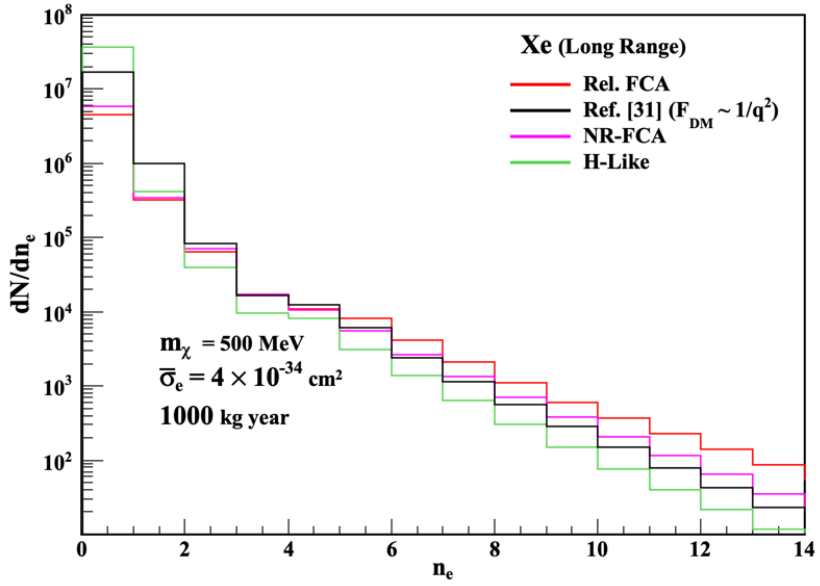

As for the long-range interaction, the low-energy cross section is so dominant that the derivation of exclusion limit is dictated by the one-electron event, i.e., the first bin. As a result, the larger event number (by about one order of magnitude) predicted in Ref. leads to a better constraint on d_1 by a similar size.

Comparisons of expected event numbers as a function of ionized electron number derived in this work (relativistic FCA, red), nonrelativistic FCA (magenta), hydrogenlike approximation (green), and from Ref. [31] (black) for Xe detectors with 1000 kg-year exposure, assuming DM mass m_χ = 500 MeV, and DM-electron interaction strengths (left) c1 = 5.28 × 10

COMPARISON OF ATOMIC APPROACHES TO CONTINUUM STATES.

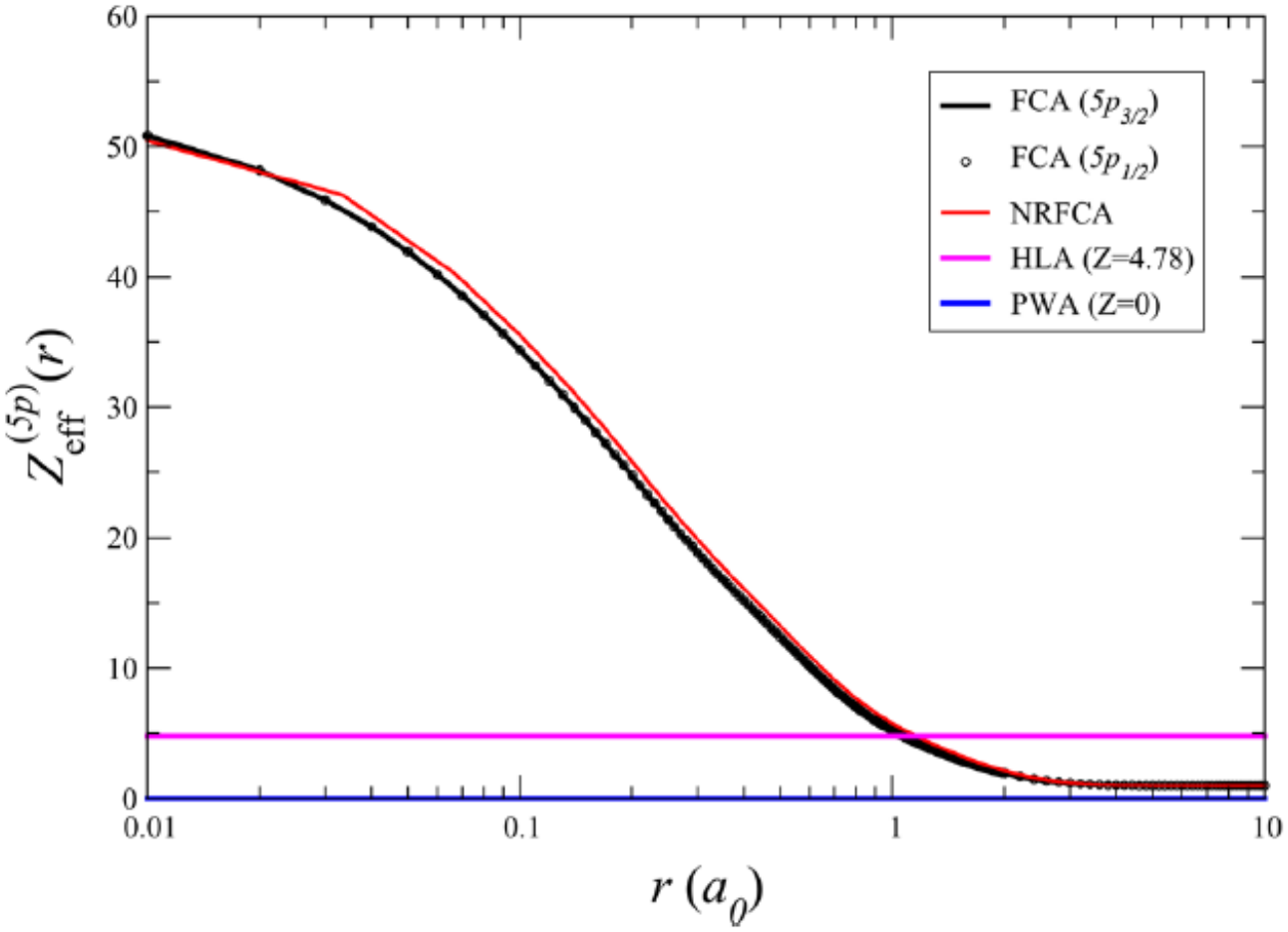

The effective charge $Z_{eff}^{(5P)}$ felt by the electron ionized from a 5p orbital derived from the approaches of FCA, NRFCA, HLA, and PWA. Note that the difference between relativistic $5p_{3/2}$ and $5p_{1/2}$ is barely visible..